

# Air quality and human health improvements from reductions in deforestation-related fire in Brazil

C. L. Reddington<sup>1</sup>, E. W. Butt<sup>1</sup>, D. A. Ridley<sup>2</sup>, P. Artaxo<sup>3</sup>, W. T. Morgan<sup>4</sup>, H. Coe<sup>4</sup> and D. V. Spracklen<sup>1\*</sup>

**Roughly 15% of the Brazilian Amazon was deforested between 1976 and 2010<sup>1</sup>. Fire is the dominant method through which forests and vegetation are cleared. Fires emit large quantities of particulate matter into the atmosphere<sup>2</sup>, which degrades air quality and affects human health<sup>3,4</sup>. Since 2004, Brazil has achieved substantial reductions in deforestation rates<sup>1,5,6</sup> and associated deforestation fires<sup>7</sup>. Here we assess the impact of this reduction on air quality and human health during non-drought years between 2001 and 2012. We analyse aerosol optical depth measurements obtained with satellite and ground-based sensors over southwest Brazil and Bolivia for the dry season, from August to October. We find that observed dry season aerosol optical depths are more than a factor of two lower in years with low deforestation rates in Brazil. We used a global aerosol model to show that reductions in fires associated with deforestation have caused mean surface particulate matter concentrations to decline by ~30% during the dry season in the region. Using particulate matter concentration response functions from the epidemiological literature, we estimate that this reduction in particulate matter may be preventing roughly 400 to 1,700 premature adult deaths annually across South America.**

Humans make extensive use of fire to clear forests and vegetation and to prepare and maintain land for agriculture<sup>8,9</sup>. Emissions of particulate matter (PM) from fires can dominate atmospheric concentrations particularly during the dry season<sup>6,10</sup>. Inhalation of PM from fires has adverse impacts on human health, including increased hospital admissions and premature mortality<sup>3,4,11,12</sup>.

Rapid deforestation is occurring across the tropics<sup>5</sup>. Between 1976 and 2010, more than 750,000 km<sup>2</sup> of the Brazilian Amazon was deforested, equivalent to ~15% of the original forested area<sup>1</sup>. Recently, Brazil has achieved well-documented reductions in deforestation rates<sup>1,5,6</sup>. Over the period 2001 to 2012, deforestation rates in Brazil declined by ~40%, from 37,800 km<sup>2</sup> yr<sup>-1</sup> in 2002–2004 to 22,900 km<sup>2</sup> yr<sup>-1</sup> in 2009–2011 (Fig. 1a;  $r = -0.71$ ,  $P = 0.005$ , trend =  $-1,390$  km<sup>2</sup> yr<sup>-1</sup>; ref. 5). The deforestation rates in the Brazilian Amazon have declined even more strongly, with reductions of 70% (refs 1,6; Supplementary Fig. 1). Reduction in deforestation rates has numerous social and environmental benefits<sup>1</sup>. We were interested in whether this reduction in deforestation rates has also improved air quality across Brazil.

Satellite-derived data sets of fire occurrence show that the total number of active fire counts across Amazonia is positively related to both deforestation rates and occurrence of drought<sup>1,7,13,14</sup>. During 2001 to 2010, years with high deforestation rates had a factor of two greater incidence of fire compared with years with low deforestation rates<sup>1</sup>. Significant declines in fire frequency across Brazil have

occurred over this period, with the largest reductions in regions of high cumulative deforestation<sup>7</sup>.

We used three different data sets of satellite-derived fire emissions<sup>2,15,16</sup> available over 2002 to 2011 (see Methods) to further explore the relationship between deforestation and PM emissions from fire. Substantial fire emissions occur across Brazil (Fig. 2), accounting for 12–16% of global particulate emissions from fire (Supplementary Table 1). In South America, particulate emissions from fire are greatest across southeast Amazonia where there is rapid deforestation (Fig. 2). Tropical forests of central Amazonia have little fire emission because high moisture, dense forest canopies and little deforestation mean that fires are a rare occurrence<sup>17,18</sup>. Regions with frequent agricultural fires also have lower total fire emission compared with regions of active deforestation, because agricultural fires result in a factor of 3–5 lower emission per unit area burned due to lower fuel loads<sup>19</sup>.

One satellite fire data set classifies emissions according to fire type<sup>2</sup>, allowing the specific contribution of deforestation fires to be estimated (see Methods). Deforestation fires account for only 20% of global total particulate fire emissions but 64% of Brazil's total, meaning that deforestation fires dominate regional air quality impacts. Classification of fire types is an uncertainty—deforestation fires may spread out of the deforested area into surrounding forest, where they are classified as a different fire type not associated with deforestation. Throughout our analysis, we therefore analyse both total particulate fire emissions and emissions specifically classified as from deforestation fires.

Over 2001 to 2011, Amazonia experienced drought conditions during 2005, 2007 and 2010 (ref. 20). We find that these drought years experienced a factor of 1.5–2.8 greater fire emission compared with non-drought years (Supplementary Table 1). The relationship between Brazil's annual deforestation rates and annual fire emissions (Fig. 1b) confirms different behaviour in drought years, consistent with analysis of fire occurrence<sup>1</sup>. We therefore focus our analysis on non-drought years, excluding 2005, 2007 and 2010.

We find significant positive relationships between Brazil's annual deforestation rates and Brazil's annual particulate fire emission (Fig. 1b) both for total fire emissions ( $r = 0.68$  to  $0.97$ ,  $P < 0.05$ ) and for emissions classified as from deforestation fires ( $r = 0.87$ ,  $P < 0.01$ ). Total particulate emissions from fire over Brazil have declined over 2002 to 2011 (Supplementary Table 1;  $r = -0.48$  to  $-0.82$ ,  $P < 0.1$ ) as have emissions from deforestation fires ( $r = -0.68$ ,  $P < 0.05$ ). Our analysis demonstrates that Brazil's fire emissions have decreased despite potential increases in agricultural fire in some regions<sup>21</sup>. Particulate emissions from deforestation fires have increased in Bolivia and Peru, but Brazil dominates total South American emissions (Supplementary Table 2). We combine data

<sup>1</sup>School of Earth and Environment, University of Leeds, Leeds LS2 9JT, UK. <sup>2</sup>Department of Civil & Environmental Engineering, Massachusetts Institute of Technology, Cambridge, Massachusetts 02143, USA. <sup>3</sup>Department of Applied Physics, Institute of Physics, University of Sao Paulo, Sao Paulo 05315-970, Brazil. <sup>4</sup>School of Earth, Atmospheric and Environmental Sciences, University of Manchester, Manchester M13 9PL, UK. \*e-mail: [d.v.spracklen@leeds.ac.uk](mailto:d.v.spracklen@leeds.ac.uk)

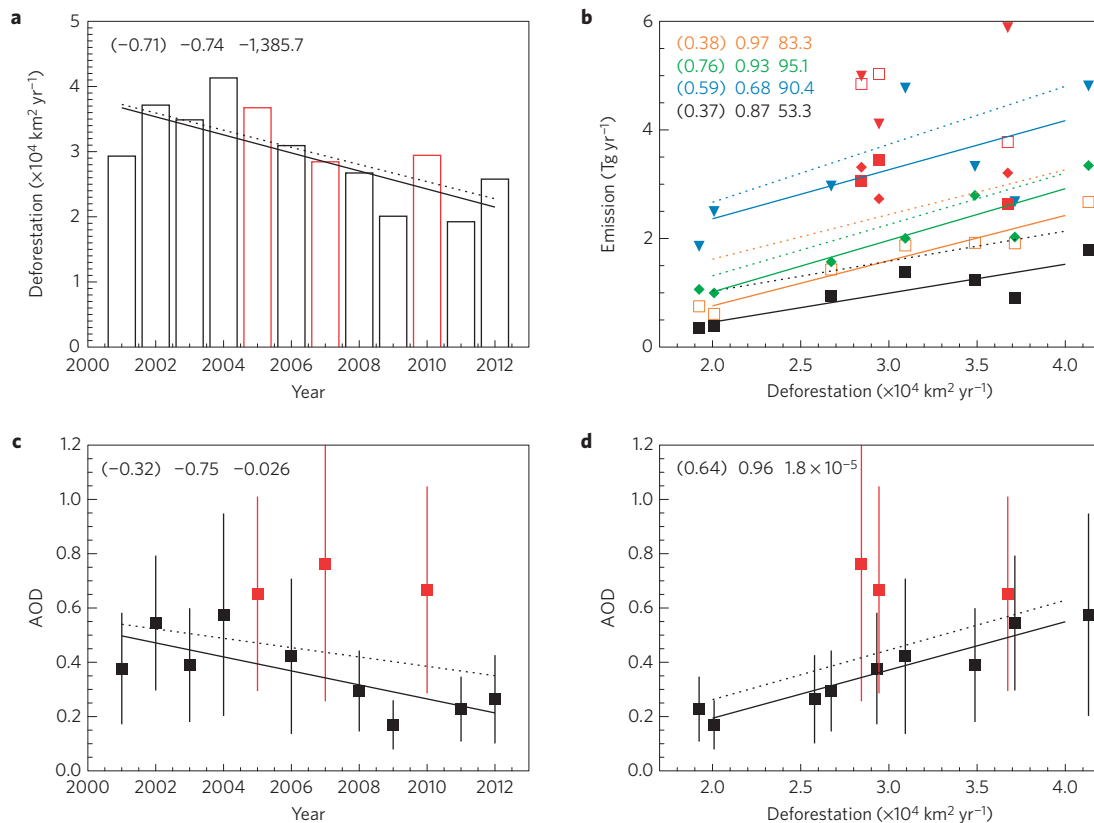


**Figure 1 | Relationships between deforestation rates, fire emissions and AOD.** **a**, Brazil's annual deforestation rates. **b**, Annual total particulate fire emission in Brazil (orange: GFED3, green: GFAS1, blue: FINN1, black: GFED3 deforestation fire) against Brazil's annual deforestation rates. **c**, Regional ( $50^{\circ}$ – $70^{\circ}$  W,  $5^{\circ}$ – $25^{\circ}$  S) dry season (August–October) MODIS AOD. **d**, Regional AOD against Brazil's deforestation rates. Drought years are indicated in red. Lines show linear relationship (solid: excludes drought years, dashed: all years). Pearson's  $r$  (all years in parenthesis) and gradient of best-fit line are detailed on each panel. Error bars (**c,d**) show standard deviation in regional daily mean AOD.

on deforestation rates with data on PM emissions from fires to calculate a regional PM emission of  $53$  to  $95 \text{ g m}^{-2}$  across Brazil (Fig. 1b), consistent with literature values for deforestation fires ( $72 \pm 30 \text{ g m}^{-2}$ ; ref. 2). Concurrent and consistent declines in Brazil's deforestation rates, fire emissions and deforestation fire emissions suggest that a reduction in deforestation fires is the primary cause of reduced particulate fire emissions across Brazil.

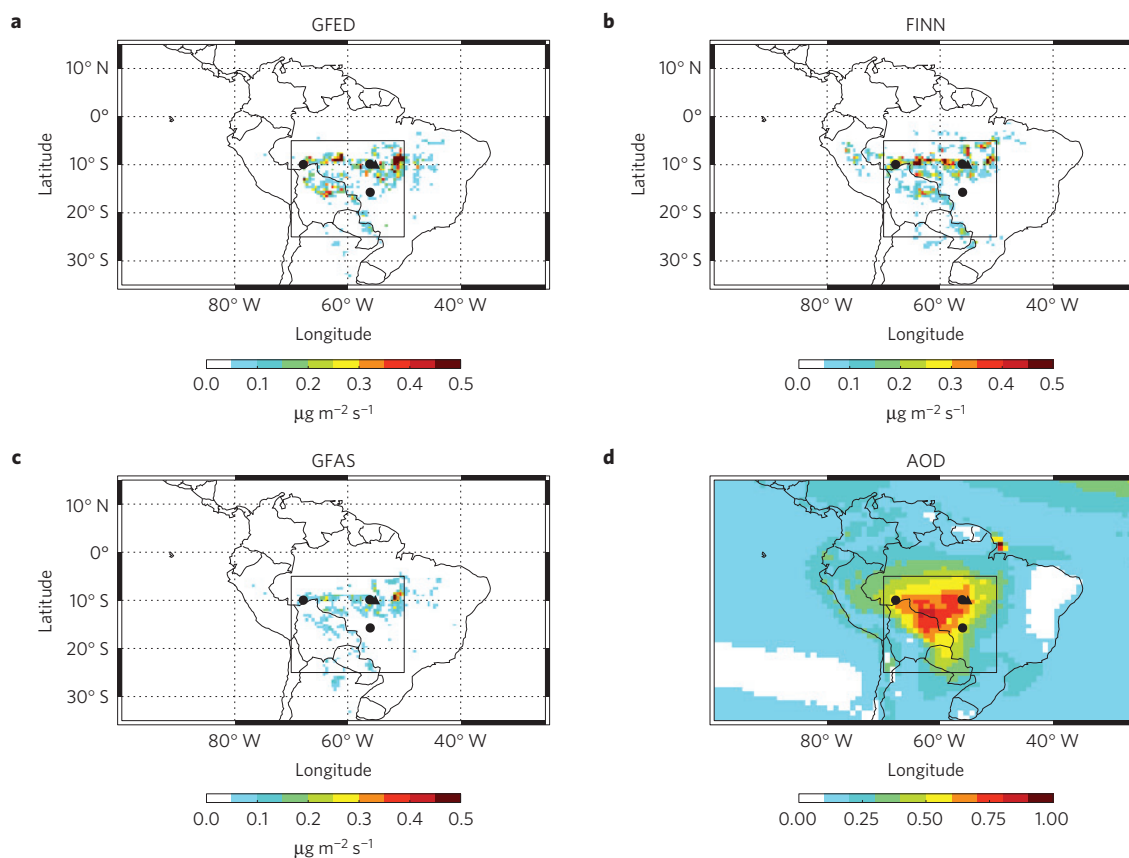
To explore whether such reductions in regional fire emissions have led to observable impacts on air quality we used multi-annual records of aerosol optical depth (AOD) from satellite and ground-based sensors. Long-term observations of surface PM concentrations are available at several sites across Amazonia<sup>6</sup>, but unfortunately no site reports over the entire period of interest. AOD is a column-integrated quantity but is related to surface PM concentrations<sup>22</sup>, so gives an indication of how PM has changed. The spatial pattern of dry season AOD retrieved by satellite (Fig. 2d) matches the locations of fires and the region of extensive deforestation in the southeast Amazon<sup>23</sup>. Atmospheric transport of smoke extends regions of high AOD over Bolivia, northern Argentina and southern Brazil, covering a large portion of South America.

Figure 1c shows observed trends in dry season mean AOD during 2001 to 2012 over the region of enhanced AOD ( $70^{\circ}$  W to  $50^{\circ}$  W,  $5^{\circ}$  S to  $25^{\circ}$  S). Fires occurring in this region account for 52–74% of total PM emissions from South American fires and so play a key role in regional air quality. Regional dry season mean AOD retrieved by satellite has declined significantly over this period ( $r = -0.75$ ,  $P < 0.01$ , AOD trend =  $-0.026 \text{ yr}^{-1}$ ), suggesting a substantial regional reduction in aerosol. Surface stations across southern Amazonia also show long-term declines in dry

season AOD (Supplementary Fig. 2; Alta Floresta,  $r = -0.65$ , Cuiaba–Miranda  $r = -0.53$ , Rio Branco,  $r = -0.50$ ), consistent with trends from satellite.

Figure 1d shows the positive relationship between observed dry season AOD and Brazil's annual deforestation rate ( $r = 0.96$ ,  $P < 0.001$ , gradient =  $1.8 \times 10^{-5} \text{ km}^{-2} \text{ yr}$ ). Years with high deforestation rates have a factor of two greater dry season AOD compared with years with low deforestation rates, suggesting that regional air quality is degraded substantially by fire emissions associated with deforestation. This link is further demonstrated by the positive relationship between observed AOD and total particulate emission from fire (Supplementary Table 1;  $r = 0.77$  to  $0.93$ ,  $P < 0.05$ ) as well as for particulate emissions from deforestation fire ( $r = 0.89$ ,  $P < 0.01$ ). Observed reductions in dry season AOD over the past decade linked to reductions in both deforestation rates and particulate emission from deforestation fires suggest that reduced deforestation may have resulted in improved air quality.

To investigate the mechanism linking deforestation rates with poor air quality, we used a global atmospheric model (see Methods). Fires increase simulated dry season surface PM<sub>2.5</sub> (particles with aerodynamic diameter  $< 2.5 \mu\text{m}$ ) across southern Brazil, Paraguay, northern Bolivia and Argentina (Fig. 3a and Supplementary Fig. 3). Deforestation fires<sup>2</sup> account for 80% of the simulated enhancement in regional PM<sub>2.5</sub> from fire, with grassland, agricultural and other fire types contributing the remaining 20% (Fig. 3a and Supplementary Fig. 3). Emissions from fires also dominate interannual variability in simulated PM<sub>2.5</sub> ( $1\sigma = 7 \mu\text{g m}^{-3}$ ) matching interannual observations of AOD ( $r^2 = 0.67$ – $0.89$ ; Supplementary Fig. 4) and PM<sub>2.5</sub> ( $r^2 = 0.41$ ; Supplementary Fig. 5).



**Figure 2 | Fire emissions and impacts on regional aerosol. a–c**, Dry season (August–October) mean emissions from fires (for 2002–2011) according to GFED3 (a), FINN1 (b) and GFAS1 (c) data sets. **d**, Dry season AOD retrieved by MODIS (for 2001–2012). The region analysed in Fig. 1 is illustrated by the black square. Circles show locations of AERONET stations; triangle shows location of PM<sub>2.5</sub> surface observations.

Without fire emissions, simulated interannual PM<sub>2.5</sub> variability is limited ( $1\sigma = 0.1 \mu\text{g m}^{-3}$ ) and comparison against observations is poor (AOD:  $r^2 = 0.02\text{--}0.34$ , PM<sub>2.5</sub>:  $r^2 = 0.08$ ), demonstrating that variability in atmospheric transport and PM deposition alone makes a minor contribution to variability in regional aerosol. Simulated dry season mean PM<sub>2.5</sub> is positively correlated with observed deforestation rates ( $r = 0.82$ ,  $P < 0.05$ ; Fig. 3a) as well as with fire emissions, both for total fire emissions (Supplementary Table 1;  $r = 0.81$  to  $0.95$ ,  $P < 0.05$ ) and for deforestation fire emissions ( $r = 0.86$ ,  $P < 0.01$ ). Years with low deforestation rates have regional dry season PM<sub>2.5</sub> concentrations that are 30% lower than years with high deforestation rates.

Our analysis demonstrates that deforestation rates and associated deforestation fires are the main drivers of observed and simulated variability in dry season aerosol loading across large parts of South America. To estimate the impacts of particulates emitted by fires on human health, we calculated the premature adult mortality from cardiopulmonary disease and lung cancer due to exposure to PM<sub>2.5</sub> from fires over the period 2002 to 2011 (see Methods). We estimate that deforestation fires alone cause an average of 2,906 premature mortalities annually across South America (95% percentile confidence interval: 1,065–4,714); 40% of the mortality due to particulate emissions from all fires over this period (Supplementary Table 3). The greatest risk to health (up to 1 mortality per 10,000 people) occurs close to deforestation fires (Supplementary Fig. 6), whereas most premature mortalities occur outside Amazonia (Supplementary Fig. 7) because of atmospheric transport of smoke to more densely populated regions.

Estimated mortality due to particulate emissions from deforestation fires is positively related to Brazil's deforestation

rates (Fig. 3b;  $r = 0.8$ ,  $P < 0.05$ , Premature mortality ( $M$ ) =  $0.071 \times$  Deforestation rates ( $D$ ,  $\text{km}^2 \text{yr}^{-1}$ )). We use this relationship to estimate that the 40% reduction in Brazil's deforestation rates is preventing 1,060 (95th percentile confidence interval: 390 to 1,720) premature adult mortalities annually across South America through reductions in deforestation fire emissions.

Our model underestimates observed AOD and PM<sub>2.5</sub> in regions impacted by fires (Supplementary Figs 4 and 5), as reported by other studies<sup>3,16</sup>. The relatively coarse resolution of global atmospheric models may contribute to underestimation of AOD. Previous studies increased fire emissions to match observations<sup>3,16</sup>, potentially accounting for fires that are not detected by satellite<sup>24</sup>. Here, we report the avoided mortalities from unscaled fire emissions as a conservative estimate of the health benefits of reduced deforestation.

Refining PM emission estimates from fire and a better understanding of the health impacts of exposure to PM (refs 25,26) are priorities for improved quantification of human health impacts from deforestation fires.

We have demonstrated that reductions in Brazil's deforestation rates have caused reduced fire emissions resulting in improved air quality with positive impacts on human health. This finding suggests that wider efforts to reduce tropical deforestation as a climate mitigation may have air quality co-benefits. To maximize these benefits, policies aimed at reducing deforestation must also minimize fire across moist tropical forests<sup>27</sup>. Decreasing deforestation may mean that fires associated with forest degradation<sup>7</sup> and agriculture<sup>21</sup> begin to dominate air quality impacts. Controlling these fire types may become increasingly important in the future. Changes to drought frequency in a future climate<sup>28</sup> will also have implications for fire emissions and future air quality. Combining rural development with a

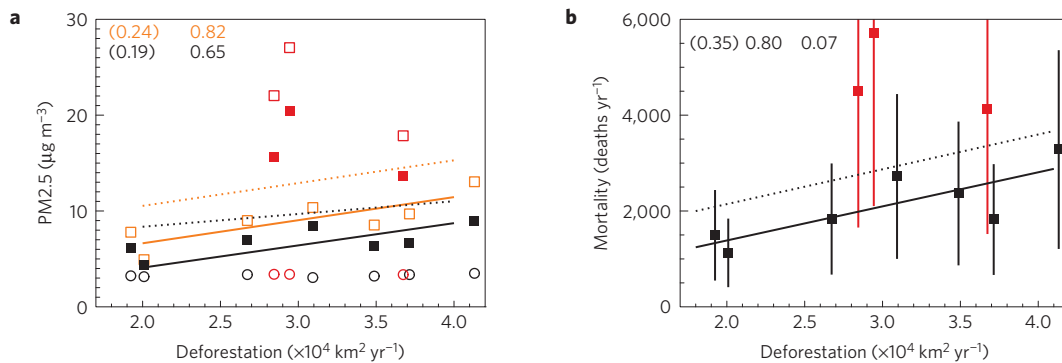


**Figure 3 | Relationship of simulated PM<sub>2.5</sub> and premature mortality against Brazil's deforestation rates.** **a**, Simulated regional (50°–70° W, 5°–25° S) dry season surface PM<sub>2.5</sub> concentrations against Brazil's deforestation rates (black filled square: GFED3 deforestation fires, orange open square: all GFED3 fire, circles: without fire). **b**, Simulated annual mortality in South America due to exposure to PM<sub>2.5</sub> from GFED3 deforestation fire emissions (error bars show 95% confidence interval). Drought years are indicated in red. Lines show linear relationship (solid: excludes drought, dashed: all years) with Pearson's linear correlation coefficient ( $r$ ) detailed on each panel (value for all years in parenthesis) and gradient of best-fit line (**b**).

low deforestation rate in Brazil will require enhanced governance<sup>29</sup>. Changes to Brazil's forest policy<sup>30</sup> may threaten recent progress in curtailing deforestation, reversing the improvements in air quality reported here.

## Methods

Methods and any associated references are available in the [online version of the paper](#).

Received 3 May 2015; accepted 13 August 2015;  
published online 16 September 2015

## References

- Aragão, L. E. O. C. *et al.* Environmental change and the carbon balance of Amazonian forests. *Biol. Rev.* **89**, 913–931 (2014).
- van der Werf, G. R. *et al.* Global fire emissions and the contribution of deforestation, savanna, forest, agricultural, and peat fires (1997–2009). *Atmos. Chem. Phys.* **10**, 11707–11735 (2010).
- Marlier, M. E. *et al.* El Niño and health risks from landscape fire emissions in southeast Asia. *Nature Clim. Change* **3**, 131–136 (2013).
- Johnston, F. H. *et al.* Estimated Global Mortality Attributable to Smoke from Landscape Fires. *Environ. Health Perspect.* **120**, 695–701 (2012).
- Hansen, M. C. *et al.* High-resolution global maps of 21st-century forest cover change. *Science* **342**, 850–853 (2013).
- Artaxo, P. *et al.* Atmospheric aerosols in Amazonia and land use change: From natural biogenic to biomass burning conditions. *Faraday Discuss.* **165**, 203–235 (2013).
- Chen, Y. *et al.* Long-term trends and interannual variability of forest, savanna and agricultural fires in South America. *Carbon Manage.* **4**, 617–638 (2013).
- Morton, D. C. *et al.* Agricultural intensification increases deforestation fire activity in Amazonia. *Glob. Change Biol.* **14**, 2262–2275 (2008).
- Cochrane, M. A. Fire science for rainforests. *Nature* **421**, 913–919 (2003).
- Pöschl, U. *et al.* Rainforest aerosols as biogenic nuclei of clouds and precipitation in the Amazon. *Science* **329**, 1513–1516 (2010).
- Jacobson, L. S. V. *et al.* Acute effects of particulate matter and black carbon from seasonal fires on peak expiratory flow of school children in the Brazilian Amazon. *PLoS ONE* **9**, e104177 (2014).
- Smith, L. T., Aragão, L. E. O. C., Sabel, C. E. & Nakaya, T. Drought impacts on children's respiratory health in the Brazilian Amazon. *Sci. Rep.* **4**, 3726 (2014).
- Aragão, L. E. O. C. *et al.* Interactions between rainfall, deforestation and fires during recent years in the Brazilian Amazonia. *Phil. Trans. R. Soc. B* **363**, 1779–1785 (2008).
- Aragão, L. E. O. C. *et al.* Spatial patterns and fire response of recent Amazonian droughts. *Geophys. Res. Lett.* **34**, L07701 (2007).
- Wiedinmyer, C. *et al.* The Fire INventory from NCAR (FINN): A high resolution global model to estimate the emissions from open burning. *Geosci. Model Dev.* **4**, 625–641 (2011).
- Kaiser, J. W. *et al.* Biomass burning emissions estimated with a global fire assimilation system based on observed fire radiative power. *Biogeosciences* **9**, 527–554 (2012).

- Bush, M. B., Silman, M. R., McMichael, C. & Saatchi, S. Fire, climate change and biodiversity in Amazonia: A Late-Holocene perspective. *Phil. Trans. R. Soc. B* **363**, 1795–1802 (2008).
- Cochrane, M. A. & Barber, C. P. Climate change, human land use and future fires in the Amazon. *Glob. Change Biol.* **15**, 601–612 (2009).
- DeFries, R. S. *et al.* Fire-related carbon emissions from land use transitions in southern Amazonia. *Geophys. Res. Lett.* **35**, L22705 (2008).
- Chen, Y., Velicogna, I., Famiglietti, J. S. & Randerson, J. T. Satellite observations of terrestrial water storage provide early warning information about drought and fire season severity in the Amazon. *J. Geophys. Res.* **118**, 495–504 (2013).
- Uriarte, M. *et al.* Depopulation of rural landscapes exacerbates fire activity in the western Amazon. *Proc. Natl Acad. Sci. USA* **109**, 21546–21550 (2012).
- van Donkelaar, A. *et al.* Optimal estimation for global ground-level fine particulate matter concentrations. *J. Geophys. Res.* **118**, 5621–5636 (2013).
- Mishra, A. K., Lehahn, Y., Rudich, Y. & Koren, I. Co-variability of smoke and fire in the Amazon Basin. *Atmos. Environ.* **109**, 97–104 (2015).
- Randerson, J. T., Chen, Y., van der Werf, G. R., Rogers, B. M. & Morton, D. C. Global burned area and biomass burning emissions from small fires. *J. Geophys. Res.* **117**, G04012 (2012).
- Burnett, R. T. *et al.* An integrated risk function for estimating the global burden of disease attributable to ambient fine particulate matter exposure. *Environ. Health Perspect.* **122**, 397–403 (2014).
- Apte, J. S., Marshall, J. D., Cohen, A. J. & Brauer, M. Addressing global mortality from ambient PM<sub>2.5</sub>. *Environ. Sci. Technol.* **49**, 8057–8066 (2015).
- Aragão, L. E. O. C. & Shimabukuro, Y. E. The incidence of fire in Amazonian forests with implications for REDD. *Science* **328**, 1275–1278 (2010).
- Malhi, Y. *et al.* Climate change, deforestation, and the fate of the Amazon. *Science* **319**, 169–172 (2008).
- Nepstad, D. *et al.* Slowing Amazon deforestation through public policy and interventions in beef and soy supply chains. *Science* **344**, 1118–1123 (2014).
- Soares, B. *et al.* Cracking Brazil's forest code. *Science* **344**, 363–364 (2014).

## Acknowledgements

This research was financially supported by FAPESP (2013/05014-0, 2012/14437-9), UBoC and the Natural Environment Research Council (NERC) through the South American Biomass Burning Analysis (SAMBBA) project (NE/J009822/1, NE/J010073/1). We acknowledge support from the LBA central office at the Brazilian National Institute for Amazonian Research (INPA), principal investigators and their staff for maintaining the AERONET sites and Google Earth Engine and team.

## Author contributions

C.L.R. performed the model simulations. P.A. provided data. C.L.R., E.W.B., D.A.R. and D.V.S. analysed the data. All authors contributed to scientific discussions and helped write the manuscript.

## Additional information

Supplementary information is available in the [online version of the paper](#). Reprints and permissions information is available online at [www.nature.com/reprints](http://www.nature.com/reprints). Correspondence and requests for materials should be addressed to D.V.S.

## Competing financial interests

The authors declare no competing financial interests.



## Methods

**Deforestation data.** Annual deforestation rates in Brazil were calculated using a Google API based on an analysis of Landsat data at a spatial resolution of 30 m over the period 2001 to 2012 (ref. 5). We compared Brazilian deforestation rates from this data set against the deforestation rates reported for the Brazilian Amazon<sup>1,6</sup> (Supplementary Fig. 1). Both data sets report a decline in deforestation between 2001 and 2012.

**MODIS aerosol optical depth (AOD).** The Moderate Resolution Imaging Spectroradiometer (MODIS) instruments on board Terra and Aqua provide AOD from 2000 to 2002, respectively through to 2012. We use the daily, gridded  $1^\circ \times 1^\circ$  product (Level 3 data) from Terra for 2001 to 2012 and Aqua for 2002 to 2012. Daytime Equator crossing is 10:30 for Terra and 13:30 for Aqua. Dry season mean (August to October) values are calculated from the combined Terra and Aqua data. We tested our analysis using Level 2 data and confirmed that this does not alter our results. Drought years (2005, 2007, 2010) have dry season AOD double that of non-drought years (Fig. 1c). Trends in dry season AOD are not significant when drought years are included ( $r = -0.32$ ,  $P = 0.15$ ), consistent with previous analysis reporting no long-term trend in AOD over this region<sup>31</sup>.

**Fire emissions.** We used three different satellite fire emission data sets: National Centre for Atmospheric Research Fire Inventory version 1.0 (FINN1; ref. 15), Global Fire Emissions Database version 3 (GFED3; ref. 2) and the Global Fire Assimilation System version 1.0 (GFAS1; ref. 16). GFED3 emissions are available from 1997 to 2011 at  $0.5^\circ \times 0.5^\circ$  resolution. FINN1 emissions are available from 2002 to 2012 at  $1 \text{ km}^2$  resolution. GFAS1 emissions are available from March 2000 to the current day at  $0.5^\circ \times 0.5^\circ$  resolution. We analysed the period 2002 to 2011 where all data sets are consistently available. We regrid all data sets to the same horizontal resolution ( $0.5^\circ \times 0.5^\circ$ ). The GFED3 data set classifies fires according to fire type<sup>2</sup>. We use the deforestation fire classification as an estimate of fire emissions associated with deforestation. Emissions from the different data sets are summarized in Supplementary Table 1.

**Rainfall.** Dry season accumulated rainfall is calculated from precipitation retrievals from the 3B42 3-h  $0.25^\circ \times 0.25^\circ$  product of the Tropical Rainfall Measuring Mission (TRMM) and other satellites. Analysis of rainfall data shows that over the regions of fires, 2007 and 2010 were particularly dry years (accumulated dry season rainfall  $> 1$  standard deviation below the 1998–2012 average). Dry season rainfall was also below average in 2005.

**Aerosol observations.** AERONET Level 2.0 (quality assured) daily average AOD retrieved at 440 nm is from three stations with 10 or more years of data: Alta Floresta (1999–2011;  $9.87^\circ \text{ S}$ ,  $56.10^\circ \text{ W}$ ), Cuiabá–Miranda (2001–2011;  $15.73^\circ \text{ S}$ ,  $56.02^\circ \text{ W}$ ) and Rio Branco (2000–2011;  $9.96^\circ \text{ S}$ ,  $67.87^\circ \text{ W}$ ). We use surface PM<sub>2.5</sub> concentrations measured using gravimetric filter analysis at a site near Alta Floresta ( $9.87^\circ \text{ S}$ ,  $56.10^\circ \text{ W}$ ) between 1992 and 2005.

**Global aerosol model.** The global distribution of PM<sub>2.5</sub> was simulated using the 3D Global Model of Aerosol Processes (GLOMAP; ref. 32), which is an extension to the TOMCAT chemical transport model. TOMCAT is driven by analysed meteorology from the European Centre for Medium Range Weather Forecasts (ECMWF), updated every 6 h and linearly interpolated onto the model time step. Model output has a horizontal resolution of  $2.8^\circ \times 2.8^\circ$  and 31 vertical model levels between the surface and 10 hPa. The vertical resolution in the boundary layer ranges from  $\sim 60 \text{ m}$  near the surface to  $\sim 400 \text{ m}$  at  $\sim 2 \text{ km}$  above the surface.

GLOMAP simulates the mass and number of size-resolved aerosol particles in the atmosphere, including the influence of aerosol microphysical processes on the particle size distribution. These processes include nucleation, coagulation, condensation, cloud processing, dry deposition, and nucleation/impact scavenging. The aerosol particle size distribution is represented using seven log-normal modes. GLOMAP treats black carbon, particulate organic matter, sulphate, sea spray and mineral dust.

Anthropogenic emissions of sulphur dioxide, black carbon and particulate organic matter are from the MACCity emissions inventory<sup>33</sup>. We complete six simulations with different landscape fire emissions: GFED3 for 1997 to 2011 with monthly emissions for 1997 to 2003 and daily emissions for 2003 to 2011; FINN1 for 2002 to 2011; GFAS1 for 2001 to 2011; no landscape fire emissions; with GFED3 emissions but with no deforestation fire emissions; with GFED3 fire emissions scaled by a factor of 3.4. We evaluated the global model with GFED3 emissions because they had the best temporal overlap with the aerosol observations.

**Analysis.** We analysed regional AOD and PM<sub>2.5</sub> over a domain covering Bolivia, southern Brazil and northern Paraguay ( $70^\circ \text{ W}$  to  $50^\circ \text{ W}$  and  $5^\circ \text{ S}$  to  $25^\circ \text{ S}$ ). Interannual variability in simulated PM<sub>2.5</sub> in this domain is correlated with MODIS AOD ( $r = 0.85$ ,  $P < 0.01$ ), confirming that our analysis of AOD gives an

indication of regional PM<sub>2.5</sub>. Particulate emissions from fires increase simulated PM<sub>2.5</sub> concentrations across our region of analysis by more than 30% for 5 months each year (June through October; Supplementary Fig. 8), meaning that the region is chronically impacted by particulate pollution from fires<sup>4</sup>.

Trends in annual forest loss, particulate emissions from fire and MODIS AOD were derived using an ordinary least-squares slope of the linear regression of the relevant parameter versus year. Relationships between different parameters (for example, AOD and deforestation rates) were also calculated using linear regression. We report the correlation as Pearson's  $r$  and calculate the significance of the relationship ( $P$ ).

**Estimation of premature mortality.** We estimate adult ( $> 30$  years) premature mortality due to long-term exposure to enhanced PM<sub>2.5</sub> concentrations from fires using concentration response functions from the epidemiological literature<sup>34</sup> that relate changes in annual mean PM<sub>2.5</sub> concentrations to the relative risk (RR) of disease. This method has been used in a number of recent assessments<sup>3,35</sup>. We estimate health impacts using annual mean PM<sub>2.5</sub> concentrations, as applied previously in studies of the health impacts of particulate emissions from fire<sup>3,4</sup>.

We used a log-linear model<sup>34</sup> to calculate RR for cardiopulmonary diseases and lung cancer following:

$$\text{RR} = \left[ \frac{(\text{PM}_{2.5,\text{control}} + 1)}{(\text{PM}_{2.5,\text{fire\_off}} + 1)} \right]^\beta$$

where  $\text{PM}_{2.5,\text{control}}$  is the simulated gridded surface annual mean PM<sub>2.5</sub> concentrations from the global model for the control experiment and  $\text{PM}_{2.5,\text{fire\_off}}$  is for the perturbed experiment without fire emissions. The cause-specific coefficient ( $\beta$ ) is an empirical parameter assumed to be 0.23218 (95% confidence interval of 0.08563–0.37873) for lung cancer and 0.15515 (95% confidence interval of 0.05624–0.2541) for cardiopulmonary diseases<sup>34</sup>. Cause-specific coefficients are derived for exposure to PM<sub>2.5</sub>, but not specifically for fire aerosol.

We calculated the attributable fraction (AF) as:

$$\text{AF} = \frac{(\text{RR} - 1)}{\text{RR}}$$

The number of excess premature mortality in adults over 30 years of age ( $\Delta M$ ) was calculated by:

$$\Delta M = \text{AF} \times M_0 \times P_{30+}$$

where  $M_0$  is the baseline mortality rate (deaths per year per head of population) for each disease risk and  $P_{30+}$  is the exposed population over 30 years of age. We used country-specific baseline mortality rates from the World Health Organisation (WHO) and human population data from the Gridded Population of the World (GPW; version 3) for the year 2010 from the Socioeconomic Data and Applications Center (SEDAC; <http://sedac.ciesin.columbia.edu/data/collection/gpw-v3>).

We calculated  $\Delta M$  at the horizontal resolution of the population data set ( $0.04^\circ$ ) for the period 2002 to 2011. We map PM<sub>2.5</sub> concentrations from the global model grid to the population grid. Calculating premature mortality at the horizontal resolution of the global aerosol model ( $2.8^\circ$ ) instead of the resolution of the population data set changes our calculated premature mortality by less than 3%. We report mortality both for all South America and separately for Brazil (Supplementary Table 3).

**Uncertainty in premature mortality estimates.** The 95% confidence interval in the cause-specific coefficients results in a factor of  $\sim 4.4$  uncertainty in estimated mortality (Supplementary Table 3). Global models with relatively coarse resolution (approximately hundreds of kilometres) typically underestimate urban-scale PM<sub>2.5</sub> concentrations. In the region surrounding São Paulo ( $46.6^\circ \text{ W}$ ,  $23.5^\circ \text{ S}$ ) GLOMAP predicts annual mean PM<sub>2.5</sub> concentrations of  $\sim 7 \mu\text{g m}^{-3}$ , matching concentrations reported by another modelling study<sup>36</sup>. Across six cities in Brazil, observed annual mean urban PM<sub>2.5</sub> concentrations range from  $7.3$  to  $28 \mu\text{g m}^{-3}$  (ref. 37). Across the same cities, annual mean PM<sub>2.5</sub> concentrations estimated by GLOMAP range from  $4$  to  $7 \mu\text{g m}^{-3}$ , with an average bias of  $-10.8 \mu\text{g m}^{-3}$  (range  $-3$  to  $-21 \mu\text{g m}^{-3}$ ). We complete sensitivity studies to assess the implications of the model underestimation of urban-scale PM<sub>2.5</sub>. We increase PM<sub>2.5</sub> concentrations in urban grid squares in both the control and perturbed (fire off) simulations, to account for missing urban-scale pollution (Supplementary Fig. 9). We use the Global Rural-Urban Mapping Project Version One (GRUMPv1) data set (<http://sedac.ciesin.columbia.edu/data/set/grump-v1-urban-extents>) to define urban grid squares. We then recalculate our health estimates using these PM<sub>2.5</sub> concentrations that are corrected for urban-scale pollution. Increasing urban annual mean PM<sub>2.5</sub> concentrations by 7, 14 and  $17 \mu\text{g m}^{-3}$  decreases our estimated premature mortality caused by exposure to PM<sub>2.5</sub> from fires by 19%, 24% and 26%,

respectively (Supplementary Table 4). Using a population density of 1,000 people km<sup>-2</sup> to define urban areas (instead of the urban definition from GRUMPv1) reduces the area we define as urban. Incrementing PM2.5 by 17 µg m<sup>-3</sup> within this urban extent reduces the premature mortality estimate by only 20%; less than the 26% we found using GRUMPv1 to define urban areas. The relatively coarse resolution of our global model therefore creates an uncertainty of ~25% in our estimated mortality from PM2.5 from fires, less than the uncertainty due to the range in cause-specific coefficients.

**Data availability.** All remote-sensed data are publicly available. Model data and PM2.5 observations are available from the authors on request.

## References

- Boys, B. L. *et al.* Fifteen-year global time series of satellite-derived fine particulate matter. *Environ. Sci. Technol.* **48**, 11109–11118 (2014).
- Mann, G. W. *et al.* Description and evaluation of GLOMAP-mode: A modal global aerosol microphysics model for the UKCA composition-climate model. *Geosci. Model Dev.* **3**, 519–551 (2010).
- Lamarque, J. F. *et al.* Historical (1850–2000) gridded anthropogenic and biomass burning emissions of reactive gases and aerosols: Methodology and application. *Atmos. Chem. Phys.* **10**, 7017–7039 (2010).
- Ostro, B. *Outdoor Air Pollution: Assessing the Environmental Burden of Disease at National and Local Levels* (World Health Organization, 2004).
- Steve, H. L. Y. *et al.* Global, regional and local health impacts of civil aviation emissions. *Environ. Res. Lett.* **10**, 034001 (2015).
- Brauer, M. *et al.* Exposure assessment for estimation of the global burden of disease attributable to outdoor air pollution. *Environ. Sci. Technol.* **46**, 652–660 (2012).
- de Miranda, R. M. *et al.* Urban air pollution: A representative survey of PM2.5 mass concentrations in six Brazilian cities. *Air Qual. Atmos. Health* **5**, 63–77 (2012).